

# Morphological changes of olivine grains reacted with amino acid solutions by impact process

HPSTAR  
473-2017

Yuhei Umeda<sup>1</sup> · Atsushi Takase<sup>1</sup> · Nao Fukunaga<sup>1</sup> · Toshimori Sekine<sup>1,2</sup> · Takamichi Kobayashi<sup>3</sup> · Yoshihiro Furukawa<sup>4</sup> · Takeshi Kakegawa<sup>4</sup>

Received: 20 April 2016 / Accepted: 24 September 2016 / Published online: 4 October 2016  
© Springer-Verlag Berlin Heidelberg 2016

**Abstract** Early oceans on Earth might have contained certain amounts of biomolecules such as amino acids, and they were subjected to meteorite impacts, especially during the late heavy bombardment. We performed shock recovery experiments by using a propellant gun in order to simulate shock reactions among olivine as a representative meteorite component, water and biomolecules in oceans in the process of marine meteorite impacts. In the present study, recovered solid samples were analyzed by using X-ray powder diffraction method, scanning electron microscopy, electron probe microanalysis, and transmission electron microscopy with energy-dispersive X-ray spectrometry. The analytical results on shocked products in the recovered sample showed (1) morphological changes of olivine to fiber- and bamboo shoot-like crystals, and to pulverized grains; and features of lumpy surfaces affected by hot water, (2) the formation of carbon-rich substances derived from amino acids, and (3) the incorporation of metals from container into samples. According to the present results, fine-grained olivine in meteorites might have morphologically changed and shock-induced chemical reactions might have been enhanced so that amino acids related to

the origin of life may have transformed to carbon-rich substances by impacts.

**Keywords** Shock recovery experiments · Marine meteorite impacts · Amino acids · Olivine · Morphological changes · Shock reactions

## Introduction

For considering the origin of life on Earth, many experiments have been conducted using different possible energy sources such as light, shock wave, discharging of electricity, heat, and high-energy beams (Aubrey et al. 2009; Furukawa et al. 2009; Kobayashi et al. 1998; Miller 1953). These experiments aim at syntheses of biomolecules related to the origin of life using minerals and source materials believed to have existed on the early Earth. Here, we have paid special attention to shock reactions caused by meteorite impacts to early Earth oceans. When hypervelocity meteorites impact the oceans, some minerals contained in meteorite may react with solutes in the oceans under high pressure and temperature conditions and subsequent pressure release processes induced after such an impact. It is likely that many extraterrestrial bodies have impacted early oceans during late heavy bombardment period (LHB) (Culler et al. 2000; Valley et al. 2002). Also, it is probable that there were considerable amounts of organic materials such as amino acids at that time (Furukawa et al. 2009; Huber and Wächtershäuser 2006; Marshall 1994; Miller 1953). Thus, it is important to investigate shock reactions between minerals and biomolecules. Especially, it has been known that hydrous minerals are formed easily under hydrothermal conditions by previous experiments (Berndt et al. 1996; Malvoisin et al. 2012; Seyfried et al. 2007).

✉ Yuhei Umeda  
yuhei-umeda@hiroshima-u.ac.jp

<sup>1</sup> Department of Earth and Planetary Systems Science, Hiroshima University, 1-3-1, Kagamiyama, Higashi-Hiroshima 739-8526, Japan  
<sup>2</sup> Center for High Pressure Science and Technology Advanced Research, Pudong 201203, Shanghai, People's Republic of China  
<sup>3</sup> National Institute for Materials Science, 1-1, Namiki, Tsukuba 305-0044, Japan  
<sup>4</sup> Department of Earth and Planetary Materials Science, Tohoku University, 2-1-1, Aoba-ku, Sendai 980-8578, Japan

Previous shock recovery experiments also have indicated that shock reactions among olivine, iron, carbon, and water form nanosized oxides and hydrous minerals such as serpentine and talc (Furukawa et al. 2007, 2011).

Recently, we have reported that biomolecules are produced in shock-recovered experiments (Furukawa et al. 2009; Umeda et al. 2016). In these experiments, mixtures of aqueous solutions and olivine powders are shocked in cavity of metal container and recovered to investigate the products as a function of shock condition. An initial mixture representing ocean, atmosphere, and meteorite is encapsulated in a metal container to retain the products. Olivine is one of the most typical minerals in ordinary chondrites that represent about 90 % of meteorites that fall on to the Earth (Krot et al. 2004). According to the previous studies, serpentine and brucite are easily formed from a mixture of olivine and water at 50 MPa at 300 °C (Malvoisin et al. 2012), depending on not only the pressure and temperature but also the grain size of olivine in the starting material and reaction time. The formation process of serpentine is promoted with increasing pH, temperature, and time (Ohnishi and Tomeoka 2007). In addition, it is known that clay minerals have affinity toward organic molecules and play an important role to concentrate organic molecules on their surface by adsorption (Hedges and Hare 1987) and to polymerize amino acids (Ferris et al. 1996).

In the present study, we investigate reactions between olivine and amino acids in water during impact process. The present results are suggestive of various reactions including Rayleigh–Taylor instability growth that displays morphology similar to the simulations by Remington et al. (2006). The morphological changes in olivine grains suggest fast crystallization from highly concentrated fluids near small olivine grains during shock process.

## Methods

### Experimental methods

A projectile (30 mm in diameter, 45 mm long), with a metal flyer (stainless steel 304, 29 mm in diameter, 2 mm thick) as illustrated in Fig. 1a, was accelerated by a propellant gun at National Institute for Materials Science (Sekine 1997). The impact velocity was measured with two pickup coils at the known distance. The details of this technique were described by Sekine (1997).

We employed natural olivine crystals from San Carlos, Arizona, with  $(\text{Mg}_{0.9}\text{Fe}_{0.1})_2\text{SiO}_4$  composition (Houlier et al. 1990) and ground them into powders used as the starting material. The sizes of most starting olivine grains were less than  $\sim 300 \mu\text{m}$ , as shown Fig. 2a. Two aqueous solutions were prepared for glycine (0.1 mol/l) and valine

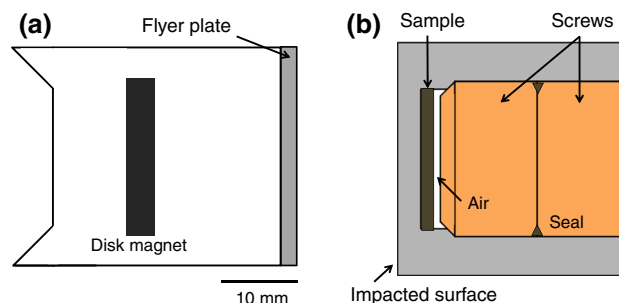


**Fig. 1** Schematic diagram of projectile (a) and sample setting in target container (b) used in the present experiments

(0.1 mol/l). Their pH values are calculated to be  $\sim 6.0$  at room temperature. Samples were set in a metal container (stainless steel 304, 30 mm in diameter and 30 mm long), as illustrated schematically in Fig. 1b. At the first step of making target, olivine powders (200 mg) were pressed by a vise and a metal rod in the sample room. Following that, a limited amount ( $130 \mu\text{l}$ ) of aqueous solution was added to the pressed olivine powders. Therefore, the pores in the pressed olivine powders were filled with the aqueous solution. A model calculation based on volume and mass shows little pore for such a sample preparation. Finally, the containers were sealed with two screws (copper, 20 mm in diameter, 12 mm long each) and were used as targets for shock recovery experiments. Gasket ring (lead) was set between screws (Fig. 1b). Before the shot, the seal condition of each sample container was checked by weight loss measurements after keeping under a vacuum for 1 h.

The experimental condition in the present study is listed in Table 1. The pressure and temperature are estimated based on the measured projectile velocity through the impedance match method and thermodynamic considerations (Furukawa et al. 2011). In shock process, the estimated peak shock pressure and temperature of sample were  $\sim 5 \text{ GPa}$  and  $\sim 250 \text{ °C}$  on average, respectively. After shock process, when the shock wave moves in the air gap, the temperature of water vapor becomes very high due to the limited volume of sample cavity. The sample container burst at higher impact velocity ( $>1 \text{ km/s}$ ). The container strength is 0.34 GPa from the fracturing experiments for container (Furukawa et al. 2011). As described in the references (Nakazawa et al. 2005; Furukawa et al. 2011), it is assumed that the gas generated in the container under shock behaves as an ideal gas. When total amount of gas in the cavity is  $7.2 \times 10^{-3} \text{ mol}$  and cavity volume is  $280\text{--}300 \text{ mm}^3$ , temperature is calculated to be  $1600\text{--}1700 \text{ K}$  under the burst condition. Therefore, the gas temperature in the present study may have reached near  $\sim 1300 \text{ °C}$ . Considering that most olivine grains did not change and that some of fine grains displayed

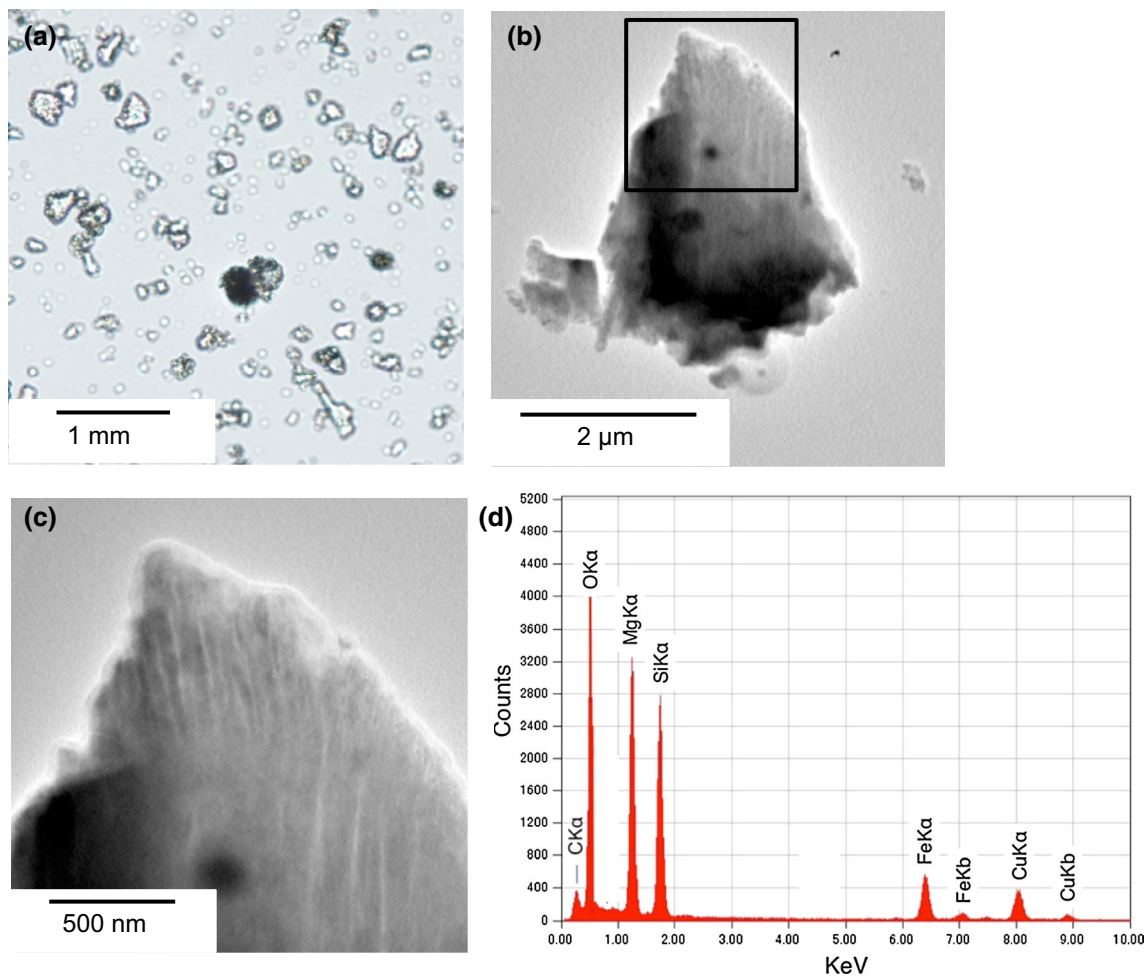


**Fig. 2** Optical microscope image (a), TEM images (b, c), and EDX spectra (d) of starting olivine grains. Image c is expansion of square in b

**Table 1** Starting materials and experimental conditions

Run no.	Starting materials (mg)			Impact velocity (km/s)	Peak shock pressure (GPa)
	Glycine 0.1 mol/L	Valine 0.1 mol/L	Olivine		
G001	130	–	200	0.81	5.0
V002	–	130	200	0.82	5.1

G001 is cited from Umeda et al. (2016)

significant morphological change, as described later, heterogeneous and local temperature rises may cause reactions under non-equilibrium. It seems to be difficult to estimate precise temperatures for reactions in the present study.

After the shots, experimental products were collected through holes (2–3 mm diameter) drilled on the impact surface of the recovered container. The details of recovery process were described by Umeda et al. (2016).

### Analytical methods

Recovered solid samples were analyzed by using optical microscopy (OM, Eclipse LV100POL; Nikon), X-ray powder diffraction method (XRD, MultiFlex; Rigaku), scanning electron microscopy (SEM, S-5200; Hitachi High-Technologies), electron probe microanalysis (EPMA, JXA-8200; JEOL), and transmission electron microscopy (TEM, JEM-2010; JEOL) with energy-dispersive X-ray spectrometry (EDX, JED-2300T; JEOL). XRD were radiated by using copper target at 40 kV and 40 mA. SEM and TEM observations were operated at acceleration voltage of 15.0 and 200 kV, respectively. Some grains were analyzed by using selected area electron diffraction (SAED) method in order to identify the respective phases. Powdered samples for SEM and EPMA analyses were carbon-coated after fixed by glue on a glass slide and polished to flat surfaces. For TEM analysis, powders were mounted on a TEM grid consisting of copper and thin carbon film.

**Fig. 3** SEM images (a) and b of samples shock-recovered from shot G001

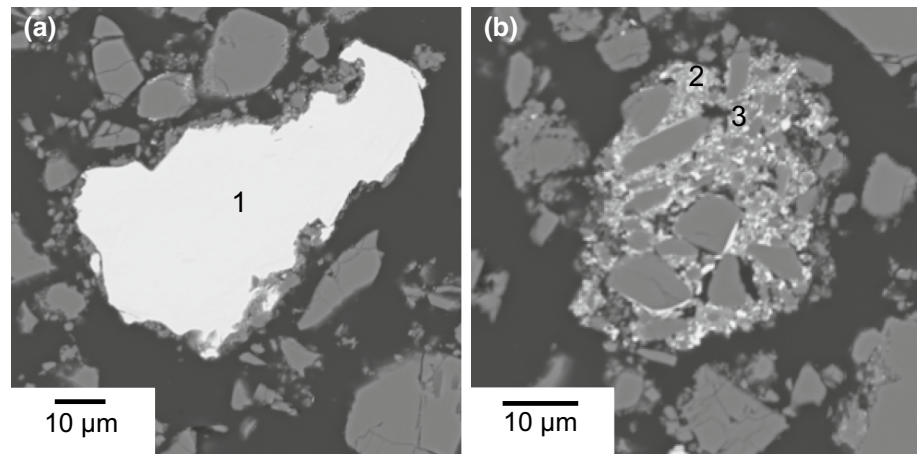


**Table 2** EPMA of major components (wt%) at points 1–7

Locations	MgO	FeO	SiO <sub>2</sub>	Fe	Cr	Ni	Mn	Total
Starting olivine	47.3	10.9	40.5	–	–	–	–	98.7
Point 1 (metal)	–	–	–	68.8	20.1	8.5	1.8	99.1
Point 2 (mixture)	9.0	1.8	7.9	59.7	12.7	7.5	1.4	100.0
Point 3 (mixture)	9.8	2.3	6.8	65.3	4.2	10.4	1.3	100.0
Point 4 (oxide edge)	50.3	9.6	41.4	–	–	–	–	101.3
Point 5 (oxide core)	48.9	9.7	40.8	–	–	–	–	99.5
Point 6 (oxide edge)	47.6	10.3	40.3	–	–	–	–	98.2
Point 7 (oxide core)	47.7	10.6	40.3	–	–	–	–	98.6

Minor components less than 0.1 wt% are ignored. EPMA data for the starting olivine (San Carlos) are from Houlier et al. (1990)

## Results

### Starting olivine

XRD analysis of the starting olivine indicated that no mineral other than olivine was present (Umeda et al. 2016). Figure 2a–c indicates results on the starting olivine particles by using OM and TEM. The grain sizes of most of the starting olivine particles were 10–300 μm (Fig. 2a). The result on EDX analysis of the starting olivine is shown in Fig. 2d. Two additional small peaks marked in Fig. 2d may be the carbon and copper of the TEM grid.

### Metallic grains in recovered samples

Figure 3a, b shows SEM images of olivine and metallic grains. EPMA results are listed in Table 2. When the total was far from 100 % at points 2 and 3 (Fig. 3b), the raw data were recalculated to be 100 % as a mixture of olivine and an alloy metal. First, a bright grain (point 1 in Fig. 3a) confirms the presence of container material. Second, some olivine grains (Fig. 3b) were aggregated and cemented, and the bright layers were <1 μm and rich in Fe, Cr, and Ni

(Table 2, points 2 and 3). These layers are agglomerates of small metal particles ejected out from the inner surface of container by shock wave. They are mixtures of olivine and stainless steel 304, with their mixing ratios of 1/4–1/5. The mass ratio of Cr/Ni at point 2 is 1.7, being similar to that of stainless steel 304 (Cr/Ni ~ 2.0), while the ratio at point 3 is 0.4. A large decrease in the Cr content may suggest that part of Cr in stainless steel 304 may have reacted out during impact process due to non-uniform shock conditions.

### Morphological changes and water reaction of shocked olivine

The recovered olivine powders were very similar to the starting olivine. A comparison of XRD patterns of olivine powders between the starting and recovered samples indicates no additional phase but significant broadenings (Furukawa et al. 2011; Umeda et al. 2016) as known grain pulverization by shock wave (Williamson and Hall 1953). Some shocked olivine grains display several types of morphological changes as observed by SEM and TEM. Figure 4a, b shows SEM images of typical grains of shocked olivine with cracks. This feature is considered to be the

**Fig. 4** SEM images of shocked olivine grains from shot G001 in EPMA analysis

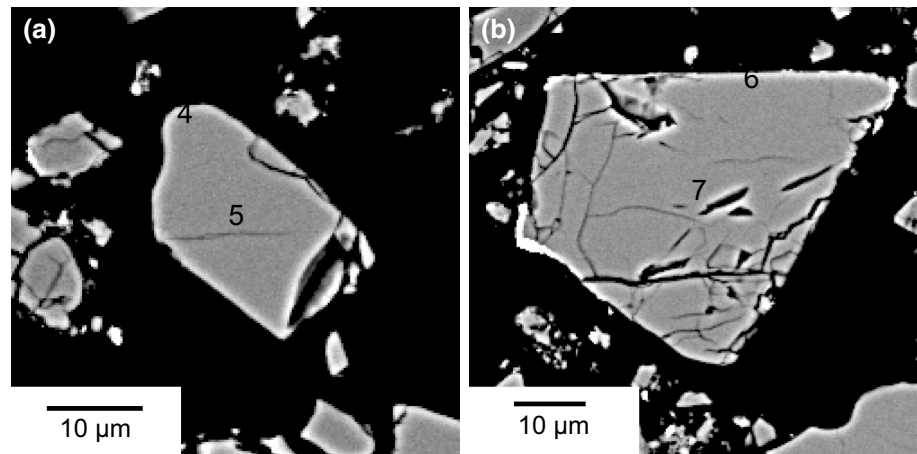
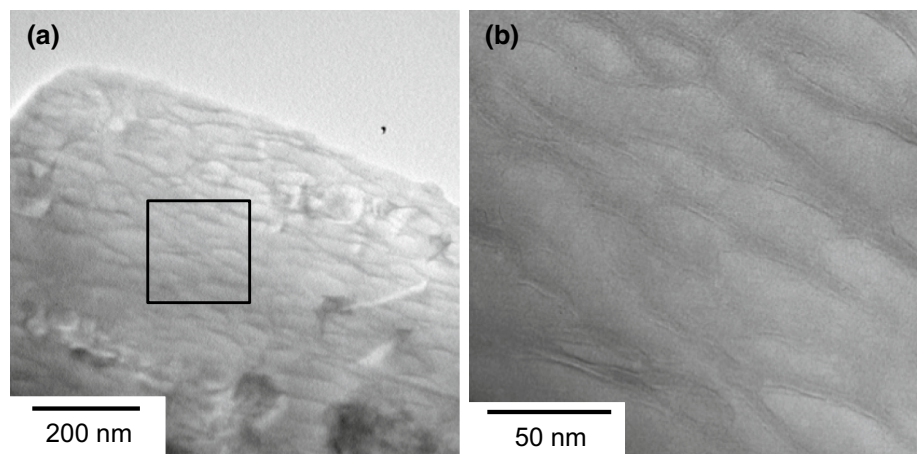


**Fig. 5** TEM images of the surface of shocked olivine from shot G001. Image **b** is an expansion of square in **a**



result of the effects of elastic shock wave. Also, in order to investigate possible hydration reactions between olivine and water, we analyzed the compositional change of olivine between core and rim. If a reaction from olivine to serpentine occurs, the atomic  $(\text{Mg} + \text{Fe})/\text{Si}$  (serpentine: 1.5, olivine: 2.0) will be smaller than that of the starting olivine. As shown in Fig. 4a, b, we analyzed edges at points 4 and 6 and cores at points 5 and 7, respectively. It seems that the edge is more reactive with surrounding water compared with the core. The ratios of  $(\text{Mg} + \text{Fe})/\text{Si}$  were 2.01 at point 4, 1.98 at point 5, 1.98 at point 6, and 1.98 at point 7, respectively. These results confirmed that the chemical compositions did not change by shock wave.

TEM observations reveal surface erosion and interaction patterns on small olivine grains, as shown Fig. 5a, b. These structures were not identified in the starting olivine grains and formed during impact process. In a previous research (Furukawa et al. 2011), shocked olivine showed a detectable deviation to serpentine and was identified as serpentine. EDX analysis of our shocked olivine for area marked by circle in Fig. 6a indicates that the peak counts ratio of

$(\text{Mg} + \text{Fe})/\text{Si}$  becomes relatively low (0.6 in Fig. 6b) compared to that of the starting olivine (1.2 in Fig. 2d). However, diffraction peaks except for that of olivine were not observed in the SAED patterns of these grains (Fig. 6c).

Several recovered olivine grains are changed morphologically, as shown Fig. 7a. In the grains covered with fiber-like materials, as shown Figs. 7a and b, there is a clear difference between crystal surfaces of the olivine grain, when one compares the changes in grain edges. The fiber-like materials are only on two edges of a rectangular-shaped crystal, as shown in Fig. 7b, but not the other edges. It suggests different reactivity by the crystal surface of the olivine. And also it is likely that smaller grains have greater reactivity with fluids than larger ones since most morphological changes are observed in grains  $<1 \mu\text{m}$ . However, such morphological changes were not present in some small grains (Fig. 7c).

### Carbon-rich substances in shocked products

There was also another type product of aggregates of fiber-like materials described in Fig. 7b. EDX results for the area

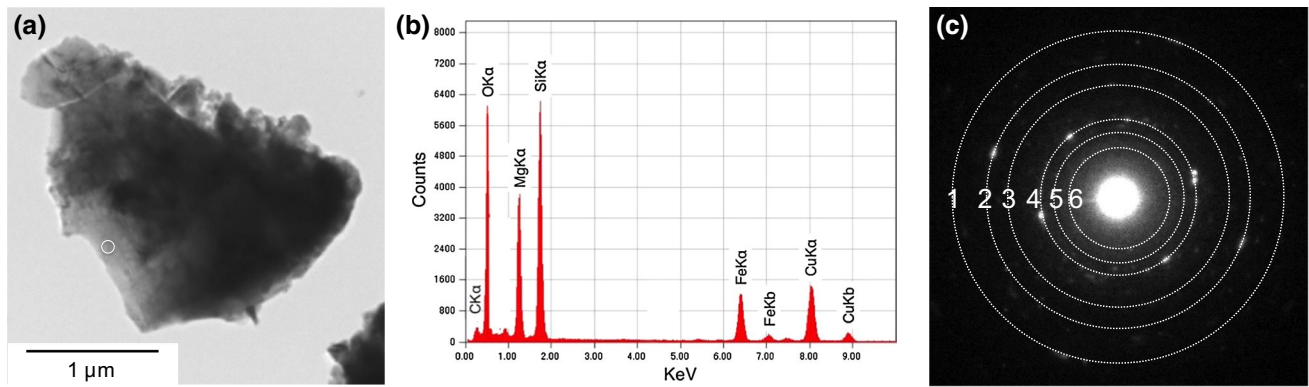


**Fig. 6** TEM image (a), EDX spectra (b), and SAED pattern (c) of shocked olivine from shot V002. Diffractions fitted in white rings 1, 5, and 6 are identified as 400, 130, and 021 planes of olivine, and

those 2–4 as 004 (or 062 or 043), 222 (or 240), and 112 (or 131) within errors, respectively

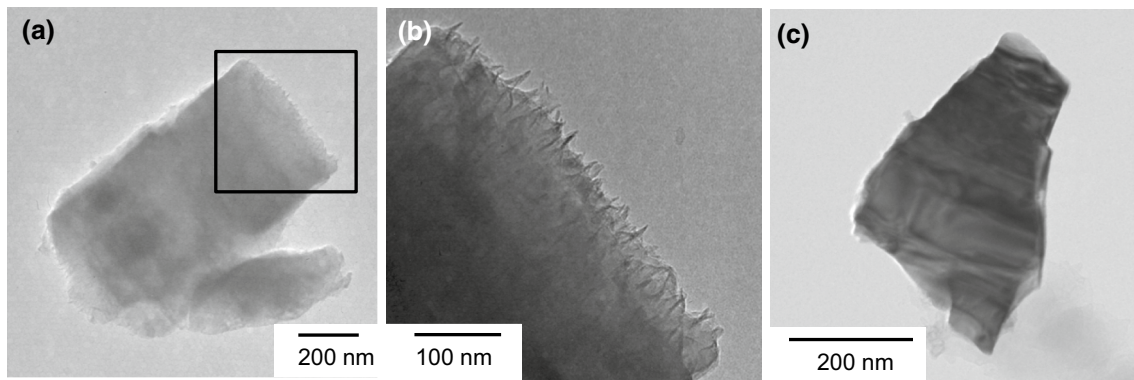


**Fig. 7** TEM images a–c of shocked olivine from shot G001

marked by circle in Fig. 8a revealed a significant amount of carbon (Fig. 8b), as well as oxygen, magnesium, and silicon. A compositional comparison with the starting olivine (Fig. 2d) suggests that the aggregate of fiber-like materials is a mixture of olivine and amorphous carbon-rich substances, because the SAED pattern for similar fiber-like materials (Fig. 8c) showed no peaks other than olivine (Fig. 8d). The amorphous carbon-rich substances may be formed as shock product from the amino acids in the starting material. These carbon-rich substances were found in both recovered samples with glycine and valine.

## Discussions

### Natural impact conditions and present experimental conditions

When flying objects of ordinary chondrite, carbonaceous chondrite, and comets impact early oceans, the impact velocities corresponding to the present study are estimated

to be 1.8, 2.2, and 2.7 km/s, respectively, based on their known Hugoniot (Umeda et al. 2016; Zhang and Sekine 2007). These impact conditions seem to be very weak in natural impacts. The impact velocity ( $\sim 1$  km/s) in the present study is an upper limit of our recovery container because the container starts to burst by gas expansion during pressure release. However, the present results may be applied for local reactions during meteorite oceanic impacts in general, although the volume fraction for such low shock pressures is significantly smaller than that of the projectile in natural impact at a typical impact velocity of  $\sim 17$  km/s (Ito and Malhotra 2006). It is because (1) the actual pressure depends on the impact angle, and low-angle impacts with high velocities generate relatively lower pressures, (2) there will be spatially weak shock areas due to being far from the impact point and locally heterogeneous pressure and temperature distributions in natural impacts even if much faster and larger meteorites impact, and (3) the prebiotic reactions might be critical at low-pressure environments. When we consider what is important for the prebiotic reactions, organic materials may decompose

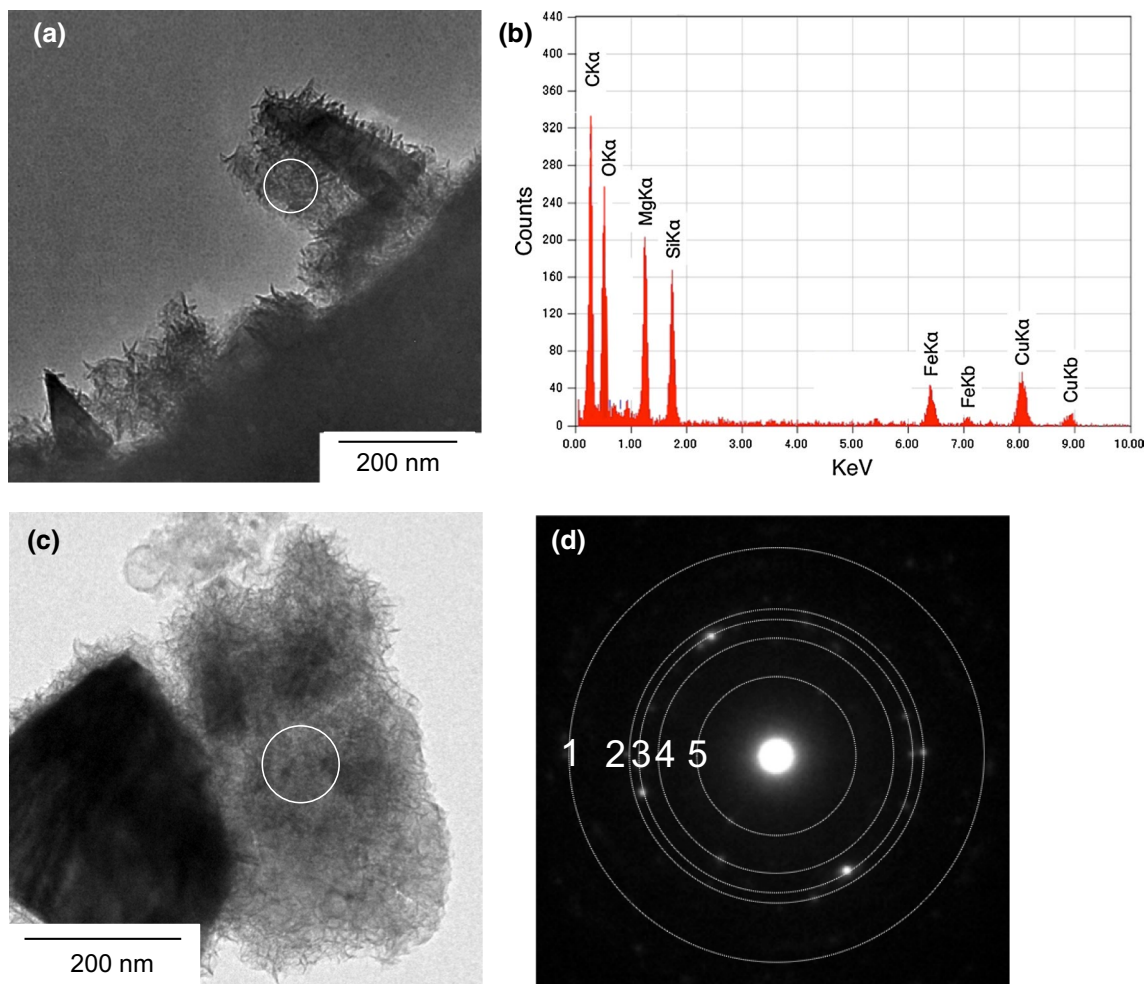


**Fig. 8** TEM image (a) and EDX spectra (b) of carbon-rich substances in recovered sample from shot G001, and TEM image (c) and SAED pattern (d) of a similar grain in recovered sample from shot

V002. Diffractions fitted in white rings 4 and 5 are identified as 130 and 021 planes of olivine, and those 1–3 as 004 (or 062 or 043), 140 (or 122), and 112 (or 131) within errors, respectively

generally at high pressures due to high temperatures for a “typical impact velocity” (e.g., Peterson et al. 1997; Blank et al. 2001). Then, the relatively low pressure may be more important even if relatively small fractions. When the experimental results are applied to low-angle oblique impacts, further considerations such as effects of the decapitation and the ricochet of the projectiles may be necessary (Schultz et al. 2006; Davison et al. 2011).

The concentration of amino acids in the present study (0.1 mol/l) is higher than the previous estimates in prebiotic oceans (de Baar and Suess 1993; Aubrey et al. 2009). Thus, the amounts of shock products such as carbon-rich substances observed in the present study might be smaller in case of natural impacts. However, our experimental conditions were relatively weaker than meteorite impact conditions, and stronger shock makes amino acid to decompose more easily. Therefore, our experimental results may be applicable although it is necessary to investigate further.

There is another issue when the present results are applied to natural impacts. Possible degassing reactions to produce CO<sub>2</sub> and NH<sub>3</sub> from amino acids may depend on whether the system is open or closed. In natural impacts it is open, but close in the present experiments. It has been known that the degassing of CaCO<sub>3</sub> depends on the available volume in shock condition (Ivanov and Deutsch 2002). In the present study, such gas phases were not analyzed, but the degassing reaction in the present condition (closed system) might be limited compared to that in the natural impact condition (open system).

### Morphological changes and water reaction of olivine

It has been known that olivine grains react with fluid water to form serpentine by shock together with mineralization of spinel and hematite (Furukawa et al. 2007, 2011). In the present study, we observed the olivine grains covered with

metal aggregates (Fig. 3b). Isolated metal grains have been involved normally in the recovered solid products (Umeda et al. 2016) due to shock-induced detachment of the inner wall of a container. The surface coating of olivine by metal may have a different mechanism. When the surface of olivine is attacked by reactive water, ferrous irons in olivine may change to metal and ferric irons. The ferric iron crystallizes as magnetite or hematite, depending on oxygen fugacity, and iron metal makes droplets, simultaneously. However, we could not confirm such reactions due to the lack of clear compositional data to support.

The lumpy surfaces of olivine grains in the recovered sample were observed (Fig. 5), as in the previous study (Furukawa et al. 2011). Present TEM observations of the recovered olivine grains (Fig. 7a) indicate fiber-like materials. EDX results for the fiber-like materials showed a compositional trend to serpentinization as proposed by Evans (2008), but they do not correspond to that of serpentine.

There are several possible reasons of different results between the present study and that of Furukawa et al. (2011). Firstly, Furukawa et al. (2011) used a method to concentrate fine particles before preparing TEM samples, and they were successful to find out serpentine. It may suggest that the amount of serpentine was very small so that we could not observe it directly. Secondly, the ratio of water content to olivine (2.6 by mass) and initial grain size (10–100  $\mu\text{m}$ ) in Furukawa et al. (2011) were different from the present study (ratio of 0.65 and grain size of 10–300  $\mu\text{m}$ ). It has been known that water contents and grain sizes have great effects on serpentinization of olivine (Malvoisin et al. 2012; Furukawa et al. 2011). According to Malvoisin et al. (2012), serpentinization rate depends strongly on initial grain size of olivine. For example, the serpentinization rate after 2000 h at 300 °C and 500 bars was 89 % for the initial grain sizes of 5–15  $\mu\text{m}$ , and only ~0.3 % for those of 100–150  $\mu\text{m}$ .

In the present study, relatively large grains (>100  $\mu\text{m}$  in size) account for more than 50 % in volume of the starting olivine powders (Fig. 2a). Although the finest grain size (10  $\mu\text{m}$ ) is similar each other, small grains (<100  $\mu\text{m}$  in size) in Furukawa et al. (2011) were more abundant than that of the present study, and their conditions for serpentinization might be more preferable than the present condition.

TEM observations of the recovered sample (Fig. 7a, b) indicate the formation of fiber-like material on the specific edges and probably high reactivity for fine grains. This trend is comparable with the result of serpentinization by hydrothermal experiments (Malvoisin et al. 2012). On the other hand, no reaction was found even in some of the similar-sized grains (Fig. 7c). The presence of such grains may provide an evidence for grain pulverization by shock wave. The pulverization is characteristic in shock process and was not observed in hydrothermal conditions. Reactivity

between olivine and fluids may also depend on the crystal planes of olivine though we could not fully investigate this yet. Especially, continual impacts of meteorite during the LHB generate highly reactive pulverized grains, and it may enhance serpentinization by repeated impacts.

The morphology of fiber-like and bamboo shoot-like crystal growths (Fig. 8a) seems to be similar to the Rayleigh–Taylor instability growth during laser ablation, as simulated by Remington et al. (2006). A shock wave transmitting the copper contacted with hydrocarbon reaches the boundary and generates interaction with each other, and a series of bamboo shoot-like growths starts in the hydrocarbon with time. When olivine and fluid water have a large density contrast and a shock wave comes out from the olivine surface, a similar situation might be realized in a limited time. Similar structures have been determined in other experimental and simulation results from laser shock compressions (Calder et al. 2002; Kane et al. 2001), as in the results by interaction between two different density liquids under shock condition (Arnett 1988; Arnett et al. 1989).

Under the post-shock condition when shock wave travels in air cavity within the sample room, a higher temperature (~1300 °C) can be generated and helps to promote reactions much effectively. Rapid crystal growth observed around solid olivine grains may indicate that an exotic condition has been achieved and that components dissolved in the fluid phase adiabatically quenched as observed fibrous surroundings. Cavity shock condition may form local density contrast in fluids between far from an olivine grain and close to it. The fluids become turbulent similar to the case where the Rayleigh–Taylor instability growth occurs during laser interactions between two materials with a large density contrast, as illustrated by simulations (Remington et al. 2006), when olivine grains act as nuclei. When crystals of  $\text{CaCO}_3$  grow in various amino acids solutions, fibrous crystals had also been observed (Xie et al. 2005). The present fiber-like crystal growth may have a similar dynamics, although our explanation is simply based on their morphological similarity and needs further characterization.

### Carbon-rich substances

The carbon-rich substances derived from amino acids were found by analytical TEM observations. Our previous study (Umeda et al. 2016) indicates ~30 mol% of the initial amino acids as the analyzed organic molecules and ~70 mol% as unknown products including carbonaceous solid products and gases. Amino acids can easily dehydrate at high temperature (Sato et al. 2004), and carbon-rich substances may contain water-insoluble peptide formed by dehydration of amino acids.

In the results of EDX analysis for an aggregate of fiber-like materials (Fig. 8b), there exists a significant amount of

carbon. Hydrogen cannot be detected in the present analysis. Nitrogen was not detected, although starting amino acids consist of atoms of C, O, N, and H. Thus, nitrogen is most likely to have removed from the amino acids during shock reaction. The discharge reaction of nitrogen from amino acids under high temperature has been known as deamination (Sato et al. 2004). Thus, ammonia and nitrogen might have been emitted as gas under the present shock conditions.

According to the present results, part of amino acids in oceans may change to carbon-rich substances due to high temperature and pressure caused by marine meteorite impacts. Amino acids have been observed in the solar system, and water-insoluble carbonaceous materials have been found in comets and meteorites (Kissel and Krueger 1987; Lawler and Brownlee 1992; Pizzarello et al. 2008). The origin and the formation mechanism of these carbonaceous materials found in extraterrestrial matters are still unknown, although they are likely to relate with the origin of life on the Earth. The present result of the formation of similar carbon-rich substance from amino acids may give new understanding of the area of astrobiology, although further investigations with a wide range of amino acid concentrations and in open systems are necessary.

Our present results suggest that considerable part of amino acid may decompose, dehydrate, and polymerize to deposit on the surface of olivine grains, though their fraction and form depend on impact condition. Further studies are needed to evaluate more details.

## Conclusions

The TEM and SEM observations of solid products shock-recovered from water–amino acid–olivine mixtures, together with elementary analyses, demonstrated the presence of morphological changes in shock-reacted olivine grains, aggregates of fiber-like materials, carbon-rich substances, and metal grains. The detected variations in the Mg/Si ratio between shock-produced fiber-like materials and the starting olivine may support a reaction to serpentinization. The results of TEM observation and EDX analysis also revealed the carbon-rich substances derived from amino acids. Fine-grained olivine in meteorite may have been reacted to make morphological changes which enhance shock reactions, and some amino acids that are related to the origin of life and initiated in early oceans may have transformed to carbon-rich substances.

**Acknowledgments** The EPMA analyses and TEM and SEM observations were performed at natural science center for basic research and development (N-BIRD), Hiroshima University. We gratefully acknowledge technical helps by K. Shibata and M. Maeda. We are thankful to T. Yamamoto for indexing of our data of SAED

patterns and K. Das for improvement of our manuscript. We appreciate reviewer's useful comments. This study was partially supported by JSPS KAKENHI Grants 24654176, 15H02144, and 15H03752.

## References

- Arnett D (1988) On the early behavior of supernova 1987A. *Astrophys J* 331:377–387
- Arnett D, Fryxell B, Muller E (1989) Instabilities and nonradial motion in SN-1987A. *Astrophys J Lett* 351:L63–L66
- Aubrey AD, Cleaves HJ, Bada JL (2009) The role of submarine hydrothermal systems in the synthesis of amino acids. *Orig Life Evol Biosph* 39:91–108
- Berndt M, Allen D, Seyfried W Jr (1996) Reduction of CO<sub>2</sub> during serpentinization of olivine at 300 °C and 500 bar. *Geology* 24:351–354
- Blank JG, Miller GH, Ahrens MJ, Winans RE (2001) Experimental shock chemistry of aqueous amino acid solutions and the cometary delivery of prebiotic compounds. *Orig Life Evol Biosph* 31:15–51
- Calder A, Fryxell B, Plewa T, Rosner R, Dupont T, Robey HF, Kane JO, Remington BA, Drake RP, Dimonte G, Zingale M, Dursi LJ, Timmes FX, Olson K, Ricker P, MacNeice P, Tufo HM (2002) On validating an astrophysical simulation code. *Astrophys J Suppl Ser* 143:201–229
- Culler TS, Becker TA, Muller RA, Renne PR (2000) Lunar impact history from <sup>40</sup>Ar/<sup>39</sup>Ar dating of glass spheres. *Science* 287:1785–1788
- Davison TM, Collins GS, Elbeshausen D, Wünnemann K, Kearsley A (2011) Numerical modeling of oblique hypervelocity impacts on strong ductile targets. *Meteorit Planet Sci* 46:1510–1524
- de Baar HJ, Suess E (1993) Ocean carbon cycle and climate change—an introduction to the interdisciplinary union symposium. *Glob Planet Change* 8:VII–XI
- Evans BW (2008) Control of the products of serpentinization by the Fe<sub>2</sub>+Mg–1 exchange potential of olivine and orthopyroxene. *J Petrol* 49:1873–1887
- Ferris JP, Hill AR Jr, Liu R, Orgel LE (1996) Synthesis of long prebiotic oligomers on mineral surfaces. *Nature* 381:59–61
- Furukawa Y, Nakazawa H, Sekine T, Kakegawa T (2007) Formation of ultrafine particles from impact-generated supercritical water. *EPSL* 258:543–549
- Furukawa Y, Sekine T, Oba M, Kakegawa T, Nakazawa H (2009) Biomolecule formation by oceanic impacts on early Earth. *Nat Geosci* 2:62–66
- Furukawa Y, Sekine T, Kakegawa T, Nakazawa H (2011) Impact-induced phyllosilicate formation from olivine and water. *Geochim Cosmochim Acta* 75:6461–6472
- Hedges JJ, Hare PE (1987) Amino acid adsorption by clay minerals in distilled water. *Geochim Cosmochim Acta* 51:255–259
- Houlier B, Cheraghmakani M, Jaoul O (1990) Silicon diffusion in San Carlos olivine. *Phys Earth Planet Inter* 62:329–340
- Huber C, Wächtershäuser G (2006)  $\alpha$ -Hydroxy and  $\alpha$ -amino acids under possible hadean, volcanic origin-of-life conditions. *Science* 314:630–632
- Ito T, Malhotra R (2006) Dynamical transport of asteroid fragments from n<sub>6</sub> resonance. *Adv Sp Res* 38:817–825
- Ivanov BA, Deutsch A (2002) The phase diagram of CaCO<sub>3</sub> in relation to shock compression and decomposition. *Phys Earth Planet Inter* 129:131–143
- Kane JO, Remington BA, Drake RP, Knauer J, Ryutov DD, Louis H, Teyssier R, Arnett D, Rosner R, Calder A (2001) Interface imprinting by a rippled shock using an intense laser. *Phys Rev E* 63:055401

- Kissel J, Krueger FR (1987) The organic component in dust from comet Halley as measured by the PUMA mass spectrometer on board Vega 1. *Nature* 326:755–760
- Kobayashi K, Kaneko T, Saito T, Oshima T (1998) Amino acid formation in gas mixtures by high energy particle irradiation. *Orig Life Evol Biosph* 28:155–165
- Krot AN, Keil K, Goodrich CA, Scott ERD, Weisberg MK (2004) Classification of meteorites. In: Davis AM (ed) *Meteorite, comet, and planets*. Elsevier, Amsterdam, pp 83–129
- Lawler ME, Brownlee DE (1992) CHON as a component of dust from comet Halley. *Nature* 359:810–812
- Malvoisin B, Brunet F, Carlot J, Rouméjon S, Cannat M (2012) Serpentinization of oceanic peridotites: 2 Kinetics and processes of San Carlos olivine hydrothermal alteration. *J Geophys Res* 117:B04102
- Marshall WL (1994) Hydrothermal synthesis of amino acids. *Geochim Cosmochim Acta* 58:2099–2106
- Miller SL (1953) A production of amino acids under possible primitive earth conditions. *Science* 117:528–529
- Nakazawa H, Sekine T, Kakegawa T, Nakazawa S (2005) High yield shock synthesis of ammonia from iron, water and nitrogen available on the early Earth. *Earth Planet Sci Lett* 235:356–360
- Ohnishi I, Tomeoka K (2007) Hydrothermal alteration experiments of enstatite: implications for aqueous alteration of carbonaceous chondrites. *Meteor Planet Sci* 42:49–61
- Peterson E, Horz F, Chang S (1997) Modification of amino acids at shock pressures of 3.5 to 32 GPa. *Geochim Cosmochim Acta* 61:3937–3950
- Pizzarello S, Huang Y, Alexandere MR (2008) Molecular asymmetry in extraterrestrial chemistry: insights from a pristine meteorite. *PNAS* 105:3700–3704
- Remington BA, Drake RP, Ryutov DD (2006) Experimental astrophysics with high power lasers and Z pinches. *Rev Mod Phys* 78:755–807
- Sato N, Quitain AT, Kang K, Daimon H, Fujie K (2004) Reaction kinetics of amino acid decomposition in high-temperature and high-pressure water. *Ind Eng Chem Res* 43:3217–3222
- Schultz PH, Sugita S, Eberhardy CA, Ernst CM (2006) The role of ricochet impacts on impact vaporization. *Int J Impact Eng* 33:771–780
- Sekine T (1997) Shock wave chemical synthesis. *Eur J Solid State Inorg Chem* 34:823–833
- Seyfried WE Jr, Foustoukos DI, Fu Q (2007) Redox evolution and mass transfer during serpentinization: an experimental and theoretical study at 200 °C, 500 bar with implications for ultramafic-hosted hydrothermal systems at Mid-Ocean Ridges. *Geochim Cosmochim Acta* 71:3872–3886
- Umeda Y, Fukunaga N, Sekine T, Furukawa Y, Kakegawa T, Kobayashi T, Nakazawa H (2016) Survivability and reactivity of glycine and alanine in early oceans: effects of meteorite impacts. *J Biol Phys* 42:177–198
- Valley JW, Peck WH, King EM, Wilde SA (2002) A cool early Earth. *Geology* 30:351–354
- Williamson GK, Hall WH (1953) X-ray line broadening from filed aluminium and wolfram. *Acta Metal* 1:22–31
- Xie AJ, Shen YH, Zhang CY, Yuan ZW, Zhu XM, Yang YM (2005) Crystal growth of calcium carbonate with various morphologies in different amino acid systems. *J Cryst Growth* 285:436–443
- Zhang F, Sekine T (2007) Impact-shock behavior of Mg- and Ca-sulfates and their hydrates. *Geochim Cosmochim Acta* 71:4125–4133